NANOSYSTEMS: PHYSICS, CHEMISTRY, MATHEMATICS, 2018, 9 (2), P. 279–289

Experimental studies of impact on a critical heat flux the parameters of nanoparticle layer formed at nanofluid boiling

V. B. Khabensky[1], A. L. Sirotkina[2], V. I. Almjashev[1,3], E. D. Fedorovich[2], V. V. Sergeev[2], V. V. Gusarov[4]

[1]A. P. Alexandrov Research Institute of Technology "NITI",
188540, Leningrad Region, Sosnovy Bor, Koporskoe shosse, 72, Russia

[2]Peter the Great St. Petersburg Polytechnic University,
195251, St. Petersburg, Politekhnicheskaya str., 29, Russia

[3]Saint Petersburg Electrotechnical University "LETI",
197376, St. Petersburg, Prof. Popov str., 5, Russia

[4]Ioffe Institute, 194021, St. Petersburg, Politekhnicheskaya str., 28, Russia

sashulena991@inbox.ru, vac@mail.ru

PACS 44.35.+c **DOI 10.17586/2220-8054-2018-9-2-279-289**

The paper presents experimental studies of nanoparticle layer, which is established on the heated surface during the boiling of nanofluid, and the influence of the process and resulting nanoparticle layer on the magnitude of critical heat flux. The examined nanofluid is distilled water (distillate) with dispersed ZrO_2 nanoparticles. A nichrome wire is used as heater. The varied parameters are: volumetric concentration of particles (C_0); exposition time in the nucleate boiling regime (τ); initial heat flux at exposition (q_0). Critical heat flux (CHF) was measured in each case. The morphology of nanoparticle layer produced in different conditions is analyzed using the method of scanning electron microscopy. The experiments have determined the influence of boiling parameters on the nanoparticle layer formation on the heated surface and sensitivity of the CHF magnitude to the properties of established nanoparticle layer in the experimental conditions.

Keywords: nanofluid, ZrO_2 nanoparticles, nanostructured surface, microstructure, departure from nucleate boiling (DNB), critical heat flux (CHF).

Received: 10 March 2018

Revised: 20 March 2018

1. Introduction

One of the main indicators of improved efficiency of heat transfer from the heated surfaces is the increased critical heat flux (CHF). Higher CHF increases thermal strength of the surface, reduces its dimensions, provides better coolant performance and improves operating reliability and safety of heat exchange equipment.

There are several ways to increase CHF: by changing the surface relief and wetting, adding surface-active agents into the coolant, though each method has inherent limitations.

Over the last 15 years, different research teams have been active in CHF studies; they examine CHF behavior at the boiling of nanoparticle (NP) water-dispersions and study their thermophysical characteristics (thermal conductivity, heat capacity, viscosity, surface tension). Main results of the studies can be found in papers and surveys (e.g. [1] and [2], respectively).

Along with the studies of CHF effects influenced by nanoparticles of different chemical composition, their concentration in the boiling coolant, heated surface geometry, NP layer morphology and other parameters, the completed research has put forward new technical solutions for the application of NP technologies for increasing CHF in the nuclear power engineering (e.g. severe accident source term mitigation in LWR); solar and space technologies, microelectronics for increasing the thermal strength and reducing dimensions of heated surfaces [3–8]. This shows the inherent utility of this technology for industrial applications.

Nanoparticles used in the fabrication of nanofluids (NF) in the CHF experimental studies were mostly based on oxides (e.g., ZrO_2, Al_2O_3, SiO_2, CuO, TiO_2 and others), different carbon formations (e.g. diamond, graphite, carbon nanotubes), carbides, also oxidation-resistant metals (e.g., gold, silver, copper).

All experiments on nanofluid boiling have registered a NP layer formation on the heated surface and, to a certain degree, the CHF increase (up to 200%) in comparison with the same at distilled water boiling.

It should be noted that the formation of a porous layer on a heater surface can take place not only upon nanofluid boiling, but also when different chemical and technological methods are applied. For example, in [9], a porous layer was synthesized, which was similar to the one produced on the heat generation components of

operating nuclear reactors. The layer was produced by the layer-on-layer deposition of particles on a substrate. The electrophoresis deposition (EPD) [10] can also be used for producing a layer having such structure.

Surface layers produced by similar methods are less heat-exchange efficient in comparison with the NP layer produced at nanofluid boiling. This is probably due to the fact that the morphology and physicochemical characteristics of the surface show the most optimal parameters only if the layer is formed during nanofluid boiling.

The following essential results have been provided by the completed experimental studies [2, 11–18]:

- Small volumetric NP concentrations in the water dispersion (0.001 – 0.1 vol. %) can cause a sufficient CHF increase.
- Thermophysical and thermodynamical properties of nanofluid, which contains small volumetric NP concentrations (heat capacity, thermal conductivity, viscosity, surface tension, density, angle of wetting on a clean surface) are practically the same as similar properties of the base liquid (for water dispersion – distilled water), and they cannot cause the CHF increase.
- At the boiling of water containing nanoparticles, the layer of these particles is established on the heated surface. It has a regular microporous structure, and its thickness grows versus the time of nucleate boiling at the rate, which increases with the growth of volumetric concentration of nanoparticles in the liquid and heat flux.
- Porous layer on the heater surface improves the wettability – reduces the wetting angle at boiling more than three-fold in comparison with the smooth steel surface, the main condition for CHF increase. This correlates to a high CHF at the distillate boiling on the surface covered by the NP layer.
- Different models have been developed to take into account the CHF sensitivity to the wetting effect; most well-known were put forward by T. G. Theofanous, T. N. Dinh [19] and S. G. Kandlikar [1]. These models give close to actual values of CHF increase at the experimental studies of nanofluid boiling, but they require the evaluated wetting angle of the NP layer, which can be determined only by experiments.

In spite of the large inventory of experimental data, the available results are ambiguous. E.g. the following is known about the influence of NP concentration on CHF: CHF increase vs. concentration growth; CHF increase vs. concentration growth to 0.01 vol.% followed by saturation; with the concentration increase a CHF grows up to a certain value, reaches its maximum and goes down. The following is known concerning the effect of NP size on CHF: the larger particle size – the smaller CHF; the correlation of CHF vs. particle size is nonmonotonic and has a maximum.

A possible reason for mentioned differences is the kinetic peculiarities of the NP layer formation, which depend on three parameters, the NP size being the same, they are: concentration of dispersed particles, magnitude of heat flux during nucleate boiling and the time of steady boiling regime. Kinetic peculiarities of the NP layer formation at the set value of these parameters determine the relief structure, its thickness and eventually the wetting angle and CHF growth.

The first experimental results on the influence of regime parameters on CHF are given in [15]: the longer period of steady nucleate boiling is accompanied by a linear growth of both NP layer thickness and CHF magnitude until saturation at the steady heat flux and different levels of NP concentration. But in [15] the inventory of experimental data is limited; the reciprocal influence of regime parameters of the NP layer thickness and relief structure, also the aggregate influence of regime parameters on the optimal characteristics of the nanoparticle layer, which provides the maximum CHF increase, is not determined.

Therefore, the objective of current work is integrated study of the effect of NF boiling regime parameters on the formation kinetics and structure of NP layer and CHF.

2. Experiments, materials and methods

At the first stage the nanofluid boiling experiments were conducted at the experimental setup having a novel design. In the experiments the nanofluid was heated to the saturation temperature in the free convection conditions. The principal schematic of the setup is shown in Fig. 1.

The setup consists of the following basic parts (Fig. 1):

- 170 ml work cell (1) – thick-walled hollow horizontal cylinder with clamp flange and glass windows to monitor the boiling process and current leads (4) having collet clamps to fix the studied heater;
- steam volume above the work cell with a thermocouple channel designed to avoid the work cell overpressurization during the experiments and for steam temperature measurements (5);
- condenser (7), in which the steam coming from the steam volume during boiling is condensed and returns into the work cell (7);

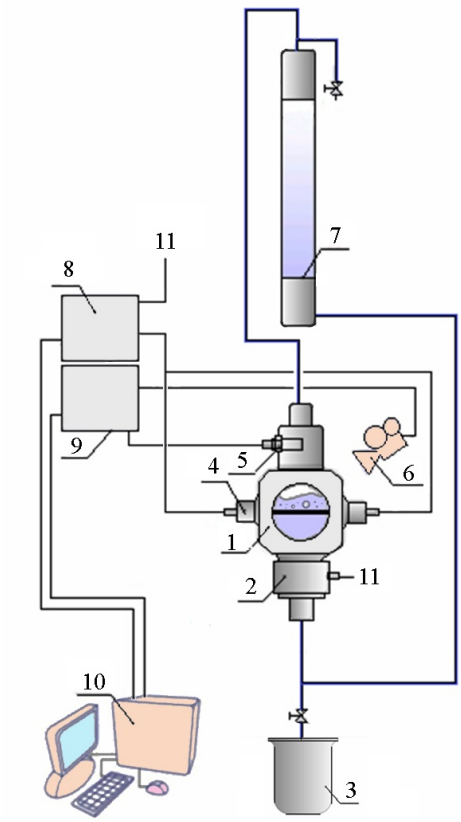

1 – work cell; 2 – preheater; 3 – drainage tank; 4 – electrodes;
5 – thermocouple channel; 6 – video camera; 7 – condenser;
8,9 – automation and measurements unit; 10 – PC; 11 – power supply

FIG. 1. Principal schematics of experimental setup

- heater (2) for the preheating of the studied fluid to the saturation temperature and its maintaining at the work cell entrance during the experiment;
- pipes and fittings for filling the work cell with a fluid and its drainage from the experimental setup;
- direct current power supply (11);
- automation and measurement unit (8, 9);
- video camera (6);
- computer (10);
- drainage tank (3).

The examined heater was a nichrome (Kh15N60 GOST 12766.1-90) wire (0.17 mm diameter).

To monitor experimental conditions, the setup included the online measurement, data acquisition and processing system. Beside that, the boiling was video-recorded through the work cell window.

The studied substance is nanofluid based on distilled water with ZrO_2 100 nm nanoparticles (manufacturer HWNANO, Hong Kong). The nanoparticle concentration in the liquid ranged from 0.001 to 0.1 vol.%. After addition of predetermined mass of nanoparticles into distilled water, the resulting dispersion was treated in an ultrasonic bath. The time of ultrasonic treatment was chosen to ensure the maximum dispersion stability. Once the dispersion was prepared, the volumetric concentration and size distribution of particles were kept under control. The period of ultrasonic exposure being optimal, if after seven days of exposition in the ambient conditions, also after several hours of boiling the nanofluid remained stable. Practically no coagulation or precipitation was observed.

The nanofluid was prepared immediately prior to each experiment. To evaluate CHF in the experimentally modelled conditions a series of calibration experiments with the distillate was conducted. At boiling on the distillate or clean surface, also at the boiling of water nanoparticle dispersions the CHF was evaluated from electric parameters at the moment of wire burnout, which was registered by the system of experimental measurements and

indicated by the data collected and processed online. Both CHF and NP layer thickness were measured in series (each combination of parameters was repeated several times).

The experiment procedure is as follows: after the experimental setup cell is filled with nanofluid, which has the preset volumetric nanoparticle concentration (from 0.001 to 0.1 vol.%), it is heated to the close to saturation temperature level; the heater is connected to power, its load corresponds to the preset initial HF level (varies in the range of 0.5 – 1.2 MW/m^2). This load level is maintained for a certain period of time – exposition time (between 1.5 – 30 min). After this, the heat flux is gradually increased in small steps up to the DNB crisis. The procedure was repeated three times in each regime; heat flux step was made shorter as the CHF was approached. The crisis is registered as the burnout of heater (wire). Corresponding value of the heat flux density is calculated as $q_{CHF} = \dfrac{U \cdot I}{\pi d L}$ (where U – voltage, V; I – current, A; d – wire diameter, m; L – length of the studied wire section, m).

This is followed by the post-test analysis of the NP layer morphology, resulting from the NF boiling on the heater in changed conditions. Nanoparticle layer thickness was evaluated in several sections along the wire length and in the two projections in the cross section close to the place of burnout. Scanning electron microscopy (SEM) was made using microscope Supra 55VP-25-78. Morphology and NP layer thickness were analyzed in the regime of secondary electrons.

Using photos provided by Supra 55VP-25-78 microscope the NP layer thickness was evaluated as the average value, to which the heater (wire) diameter increases in several locations.

3. Results and discussion

3.1. Experimental data on the CHF evaluation

Figures 2–5 provide experimental results on the evaluation of relative CHF changes in NF, when different parameters in the $q_{cr}^{nf}/q_{cr}^{dist} = f(q_0, C_0, \tau)$ coordinates were changed, where q_{cr}^{nf} – CHF in NF; q_{cr}^{dist} – CHF in the distilled water; C_0 – volumetric concentration of NP, vol.%; τ – exposition time in the boiling regime at q_0 heat flux; q_0 – initial heat flux value, MW/m^2.

The error given in Figs. 2–5 was calculated as the standard uncertainty (standard deviation) in the measurement series for each combination of parameters.

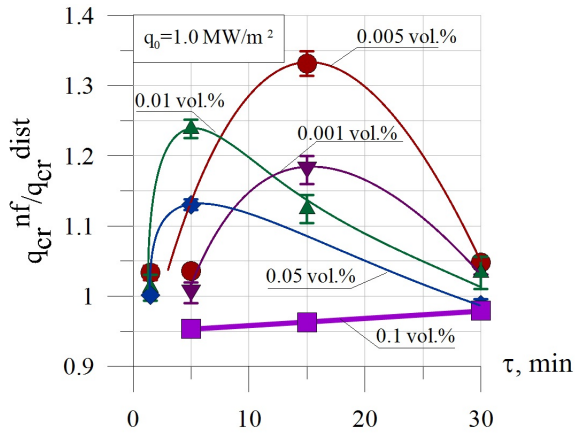

FIG. 2. $q_{cr}^{nf}/q_{cr}^{dist}$ versus exposition τ for different volumetric concentrations of nanoparticles C_0 at initial heat flux $q_0 = 1.0$ MW/m^2

Experimental data on the evaluation of $q_{cr}^{nf}/q_{cr}^{dist}$ given in Figs. 2–5 show the following:

1. Increase in the value of one of the above-given parameters, others kept the same, first leads to the growth of relative critical heat flux ($q_{cr}^{nf}/q_{cr}^{dist}$), it goes down after the maximum CHF level is reached.

2. At this, when one of the three parameters (q_0, C_0, τ) is varied and two others are kept constant, $q_{cr}^{nf}/q_{cr}^{dist}$ gets the maximum value, which corresponds to practically same values of ($q_0^{\max}$, $C_0^{\max}$, $\tau^{\max}$).

3. E.g. at $q_0 = 1.0$ MW/m^2, $C_0 = 0.01$ vol.% and $\tau = 5$ min we have:

- in Fig. 2 and Fig. 5 at fixed values of $q_0 = 1.0$ MW/m^2, $C_0 = 0.01$ vol.% and τ varying, the maximum $q_{cr}^{nf}/q_{cr}^{dist} = 1.25$ is reached at $\tau = 5$ min;

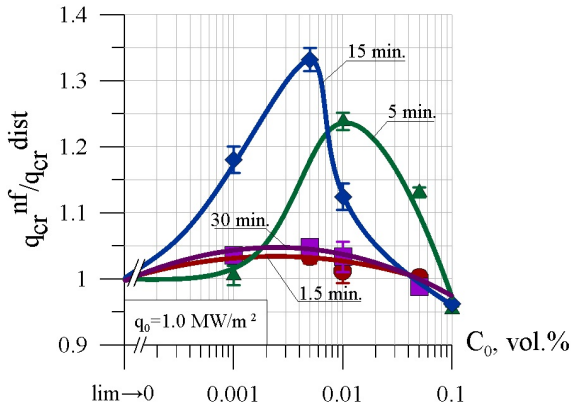

FIG. 3. $q_{cr}^{nf}/q_{cr}^{dist}$ versus volumetric concentration NP C_0 for different expositions τ at initial heat flux $q_0 = 1.0$ MW/m^2

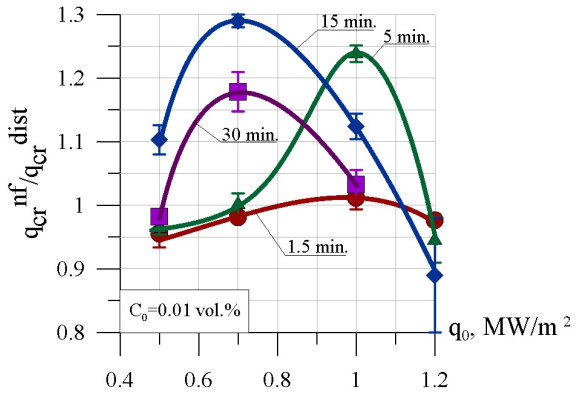

FIG. 4. $q_{cr}^{nf}/q_{cr}^{dist}$ versus initial heat flux q_0 for different expositions τ at the volumetric nanoparticle concentration $C_0 = 0.01$ vol.%

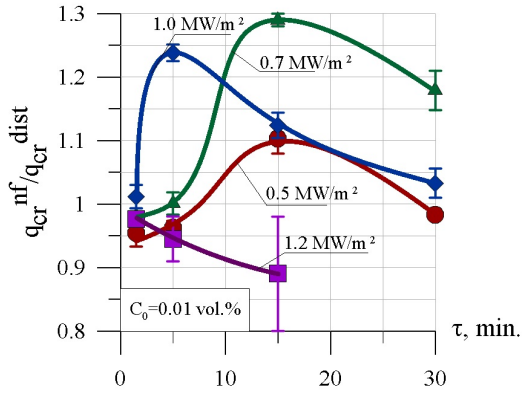

FIG. 5. $q_{cr}^{nf}/q_{cr}^{dist}$ versus exposition τ for different initial heat flux values q_0 at the volumetric nanoparticle concentration $C_0 = 0.01$ vol.%

- in Fig. 3 at fixed values of $q_0 = 1.0$ MW/m^2, $\tau = 5$ min and C_0 varying the maximum value of $q_{cr}^{nf}/q_{cr}^{dist} = 1.25$ is reached at $C_0 = 0.01$ vol.%;
- in Fig. 4 at fixed values of $C_0 = 0.01$ vol.%, $\tau = 5$ min and q_0 varying the maximum value of $q_{cr}^{nf}/q_{cr}^{dist} = 1.25$ is reached at $q_0 = 1.0$ MW/m^2.

Therefore, as the increase of any parameter leads to the NP layer thickness growth, the $q_{cr}^{nf}/q_{cr}^{dist}$ maximum value reached at the same parameter values can indicate the following: first, close to linear influence of each parameter on the NP layer thickness; and second, maximum value of $q_{cr}^{nf}/q_{cr}^{dist}$, with a high probability, corresponds to the determined optimal thickness and morphology of ZrO_2 nanoparticle layer, which ensures the smallest wetting angle, insignificant thermal resistance and open porosity, which is sufficient for the capillary water supply.

3.2. Morphology of nanoparticle layer

To analyze the morphology of NP layer, which was produced on the boiling surface at different regimes and parameters, and to determine its influence on CHF the following SEM studies of samples were conducted.

Analysis of the X-ray diffraction data and SEM images has shown that the size of the main fraction of ZrO_2 nanoparticles used in the experiment is about 100 nm, but there is a finer-grain fraction present, which has <100 nm particles. Analysis of the nanopowder's elemental composition made by EDX analysis gives the following: 76.7 mass % zirconium, 21.6 mass % oxygen; the sample also contains 1.7 mass % hafnium, which corresponds to the solid solution of hafnium dioxide in zirconia. The X-ray diffractometry of nanopowder also provides evidence that the main phase of the examined powder is the monoclinic modification of ZrO_2.

In order to analyze the influence of NP layer relief on CHF, let us consider the relief changes vs. its thickness. As an example, we consider surface relief versus the exposition time extension at the same NF concentration and unchanged initial heat flux. Fig. 6 shows images of the NP layer relief, which was produced by changing the exposition time at nanofluid concentration $C_0 = 0.01$ vol.% and initial heat flux $q_0 = 1.0$ MW/m^2. In this case the maximum CHF occurs at the exposition time $\tau = 5$ min (Fig. 6b). The ZrO_2 nanoparticle layer has a rather regular roughness with a distance between the neighboring nanoparticle aggregate peaks of 1.5–2.5 μm.

IIt is evident from Fig. 6 that as the exposition time increases, the surface relief changes. After the 1.5 min exposition, it is homogeneous, microregular with a relatively uniform combination of peaks and hollows. At the 5 min exposition the relief continues to be homogeneous and microregular, but, as a result of grown thickness of NP layer the hollow is deeper, which can make the wetting angle smaller. As is evident from Figs. 2–5, at the 5 min exposure, the maximum value of $q_{cr}^{nf}/q_{cr}^{dist}$ is reached. Further exposition to 15 min and 30 min makes the relief of NP layer irregular; it has different thicknesses and microstructure. The growth of NP layer thickness increases its thermal resistance. Both factors contribute to the considerable CHF decrease, up to $q_{cr}^{nf}/q_{cr}^{dist} \approx 1$.

Therefore, it can be assumed that there exists an optimal NP layer thickness, which corresponds to the highest CHF.

The completed SEM analysis of the wire samples after the CHF was reached also confirmed the assumption given in Section 3: close to linear correlation between the NP layer thickness growth character at changes in one of the given parameters (q_0, C_0, τ), the other two kept steady. Fig. 7 gives the NP layer thickness versus changing one of the three parameters.

It can be seen from Fig. 7a,b,c that at changing one of the parameters and getting in each case values of $q_0 = 1.0$ MW/m^2, $C_0 = 0.01$ vol.% and $\tau = 5$ min, the NP layer thickness stays unchanged and corresponds to ≈ 2 μm. At this, Figs. 2 and 5 show that in the mentioned parameter values the $q_{cr}^{nf}/q_{cr}^{dist}$ gets its maximum. This is an indirect proof of an optimal thickness of NP layer, at which the CHF is at its maximum.

Statistical analysis of experimental data (71 measurements) is represented on Fig. 8. Residual dispersion is 0.0315, standard uncertainty is 0.0214. Therefore, we can conclude that data scattering is less than 5 %. High values of scattering for measurements with low heat flux levels could be due to sufficient irregularity of nanoparticles layer thickness with high nanofluid concentration and long boiling time.

The limited inventory of experimental data and inherent properties of experimental facility (small volume of work cell, small diameter of heater – 0.17 mm-diameter wire) and a rather big size of nanoparticles ($\sim$ 100 nm) does not allow a detailed study of the changed nanoparticle layer morphology and geometric parameters of the cells – steam generation centers – versus the thickness of NP layer and CHF sensitivity to them. These data are critical for the numerical model development. However, the provided qualitative relationships provide well-grounded conclusions.

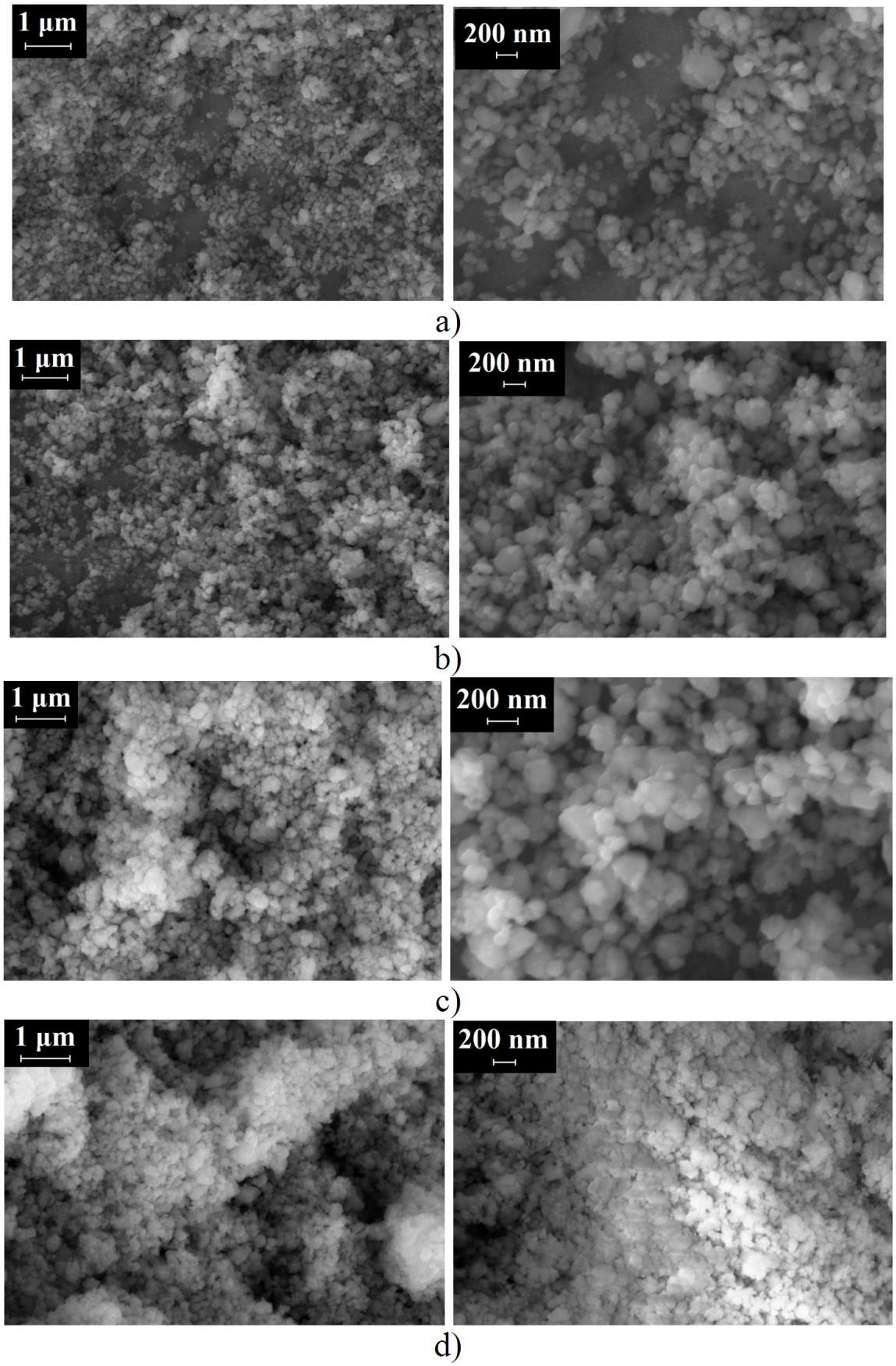

FIG. 6. Surface relief changes versus the longer exposition time (concentration 0.01 vol.%, initial heat flux 1.0 MW/m^2) a) $\tau = 1.5$ min; b) $\tau = 5$ min; c) $\tau = 15$ min; d) $\tau = 30$ min

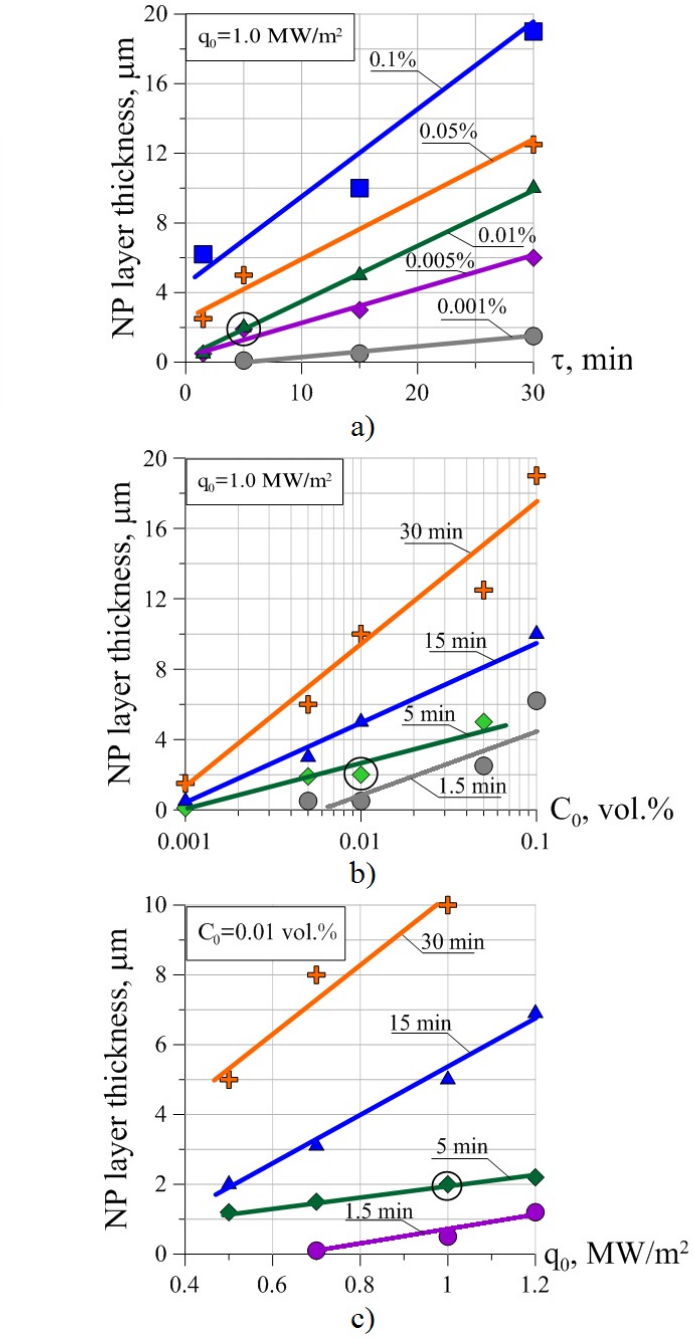

FIG. 7. NP layer thickness (μm) versus boiling parameters: a) at $q_0 = 1.0$ MW/m^2, changed τ (min) for different C_0 (vol.%); b) at $q_0 = 1.0$ MW/m^2, changed C_0 (vol.%) for different τ (min); c) at $C_0 = 0.01$ vol.%, changed q_0 (MW/m^2) for different τ (min). Black circle indicates points with coordinates $C_0 = 0.01$ vol.%, $q_0 = 1.0$ MW/m^2, $\tau = 5$ min, which corresponds to the maximum CHF value

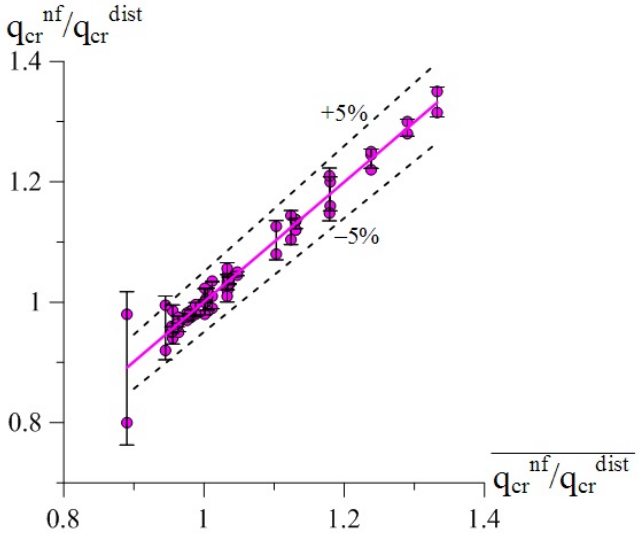

FIG. 8. $q_{cr}^{nf}/q_{cr}^{dist}$ variation against average value of this parameter in all experimental data

4. Result discussion

Completed experimental studies have determined the following qualitative relationships for the relevant conditions and parameter ranges:

1. If one of the three parameters (q_0, C_0, τ) is increased, and two others stay fixed, the critical heat flux ($q_{cr}^{nf}/q_{cr}^{dist}$) on the heated surface covered with a layer of ZrO_2 nanoparticles grows, gets its maximum value and decreases.

2. Each combination of (q_0, C_0, τ) parameter values has its maximum value of ($q_{cr}^{nf}/q_{cr}^{dist}$), which is fixed irrespective of the varied specific parameter.

3. Thickness of nanoparticle layer on the heated surface grows following the close to linear curve with an increase of any parameter (q_0, C_0, τ).

4. For each combination of (q_0, C_0, τ) parameter values the ($q_{cr}^{nf}/q_{cr}^{dist}$) maximum is reached at an approximately the same optimal thickness of NP layer (2 μm), irrespective of the varied parameter.

We can assume that the experimentally observed pattern of CHF dynamics (initial growth to maximum followed by decrease) at the increased NP layer thickness was caused by the changes in geometric characteristics of the cells – steam generation centers, and in the NP layer morphology.

In the publication [2] discuss the dependence of wetting angle, the nanolayer morphology being regular, on geometrical characteristics of cells (distance between the vertices and pits) formed at boiling. The cells are steam generation centers, which make a critical contribution into the wetting angle magnitude and, consequently, determine the tear-off diameter of the bubble and CHF.

We can propose the following mechanism of changing wetting angle and CHF. If one of the parameters (C_0, q_0 and τ) changes at nanofluid boiling, the NP layer thickness grows linearly. In the early period of the NP layer growth the surface continues to keep regular morphology and the ratio between the mentioned geometric characteristics of cells (steam generation centers) changes. This results in the decrease of wetting angle and tear-off diameter of the bubble and to the growth of CHF. When the NP layer grows to a certain thickness, the ratio of cell geometric parameters reaches an optimal value, which corresponds to maximum CHF. With further growth of the NP layer thickness the ratio between geometric parameters of the cell – steam generation center reduces. At this, the regularity of the NP layer morphology starts to decay. These factors cause the wetting angle increase and CHF reduction. It is evident that the NP layer thickness is the integral parameter, which determines the character of CHF changes, when any of the regime parameters is changed.

We should mention another important experimental result produced within this work. In all situations, when one of the regime parameters was varied (C_0, q_0 and τ), the maximum CHF occurred at the same NP layer thickness, which was ~ 2 μm. If the detailed examination proves that the same NP layer thickness corresponds to the maximum CHF, and the known linear speed of NP layer thickness growth when one of the regime parameters

is changed, we can get the optimal NP layer morphology (in terms of heat transfer characteristics). We also can model the optimal morphology using other methods.

The mentioned relationship patterns bring a number of conclusions for practical application. Here are some examples.

When nanofluids are used as coolants in the boiling type systems, as recommended in some publications, the NP layer thickness increases and, with time, the heat transfer efficiency is lost both for the CHF and heat exchange at boiling. For this reason, a positive effect of the NP layer is possible only in case of distilled water boiling.

A number of works studying the influence of volumetric concentration of nanoparticles on CHF gave different sensitivity of CHF vs. C_0 for nanoparticles of the same type. This can be a consequence of the methodology and experimental specifications. For example, if we set constant values of the initial heat flux (q_0) and exposition time (τ), when the volumetric NP concentration (C_0) is varied, the CHF is evaluated at different NP layer thicknesses, which, in the end, determines the different character of CHF versus C_0 correlations. But, in accordance with experimental data given in the paper, there should be no influence of volumetric NP concentration on the CHF, if we consider the CHF dependence on the NP layer thickness. These considerations also show low efficiency of a high volumetric concentration of nanoparticles in the dispersion (> 0.5 vol.%) on the CHF, as a fast growth of the NP layer thickness to the beyond optimal value cannot ensure a significant CHF increase.

Heat exchange at nanofluid boiling was beyond the presented research study. Anyway, the provided correlations and patterns can be used for qualitative estimate of the possible ambiguous behavior of heat transfer coefficient at boiling on the surface covered with NP layer, depending on the layer thickness. We can assume that at the NP layer corresponding to the increased CHF, the heat transfer coefficient will increase in comparison with the boiling on the clean surface, because the wetting angle is smaller (tear-off diameter of the bubble) and low thermal resistance (as the NP layer thickness is less than 2 μm, at $q = 1$ MW/m^2, $\Delta t \leq 1$ °C). It will get the highest value at maximum CHF. When the NP layer grows to ~ 8 μm the heat transfer coefficient can decrease sufficiently in comparison with the heat exchange at boiling on a clean surface because of the wetting angle increase (larger tear-off diameter of the bubble) and considerable increase of thermal resistance (NP layer thickness 8 μm, at $q = 1$ MW/m^2, $\Delta t \approx$ 4–5 °C).

5. Conclusions

The completed experimental studies of nanoparticle layer formation in a boiling nanofluid have identified a number of patterns and correlations related to the influence of nanolayer thickness on the critical heat flux. Using the provided patterns, a qualitative analysis has been made. It examined peculiarities of the CHF behavior versus the NP layer thickness; influence of regime parameters (C_0, q_0 and τ) on the CHF value; restrictions of the experimental methodology and specifications in the studies of the CHF sensitivity to regime parameters; characteristic NP layer thickness at the maximum CHF; influence of the NP layer thickness on the heat transfer coefficient at the nanofluid boiling in comparison with the heat transfer coefficient at the boiling of distilled water on the smooth surface.

Unfortunately, a rather small volume of the work cell, small diameter of the heating element and a rather big size of nanoparticles restrict the possibilities for obtaining detailed quantitative information on the structure and geometric characteristics of the nanoparticle layer, also understanding of the influence of these parameters on the wetting angle and thermal characteristics (CHF and heat transfer coefficient) versus the NP layer thickness.

In order to analyze the possibility of extrapolatory scaling of the experimental data, it is necessary to make dedicated experiments on a series of experimental facilities with different heated surfaces and nanoparticles of different size and composition. In the context of determining heat transfer characteristics and CHF, of highest importance are the studies of the wetting angle and geometric parameters of cells – steam generation centers versus the nanoparticle layer thickness, especially in the vicinity of maximum CHF.

Acknowledgements

The authors would like to thank I. K. Boricheva for help in SEM analysis and A. V. Lysenko for technical assistance.

References

[1] Kandlikar S.G. A theoretical model to predict pool boiling CHF incorporating. *International Journal of Heat and Mass Transfer*, 2001, **123**, P. 1071–1079.

[2] Truong B., Hu L.-W., Buongiorno J. Optimizing Critical Heat Flux Enhancement Through Nanoparticle-Based Surface Modifications. *Proceedings of ICAPP'08*: Paper 8209, Anaheim, CA USA, 2008, P. 1699–1706.

[3] Kim H., Buongiorno J., Hu L.-W. [et al]. Experimental study on quenching of small metal sphere in nanofluids. *Proceedings of IMECE 2008*. Paper 67788, Boston, MA USA, 2008.
[4] Kim H., Buongiorno J., Hu L.-W., McKrell T. Nanoparticle deposition effects on the minimum heat flux point and quench front speed during quenching in water-based alumina nanofluids. *International Journal of Heat and Mass Transfer*, 2010, **53**, P. 1542–1553.
[5] Chinchole A.S., Kulkarni P.P., Nayak A.K. Experimental investigation of quenching behavior of heated zircaloy rod in accidental condition of nuclear reactor with water and water based nanofluids. *Nanosystems: Physics, Chemistry, Mathematics*, 2016, **7**(3), P. 528–533.
[6] Chupin A., Hu L.-W., Buongiorno J. Applications of nanofluids to enhance LWR accidents management in in-vessel retention and emergency cooling systems. *Proceedings of ICAPP'08*. Paper 8043, Anaheim, CA USA, 2008, P. 1707–1714.
[7] Bang I.Ch., Jeong J.H. Nanotechnology for advanced nuclear thermal-hydraulics and safety: boiling and condensation. Nuclear engineering and technology, 2011, **43**(3), P. 217–242.
[8] Barrett T.R. Investigation the use of nanofluids to improve high heat flux cooling systems. *Fusion Engineering and Design*, 2013, **88**(9-10), P. 2594–2597.
[9] Buongiorno J. et al. *Synthesis of CRUD and its Effect On Pool and Subcooled Flow Boiling*. CASL L3 Milestone Report. US Department of Energy, 2015.
[10] Corradini M., Marschman S., Goldner F. *Improved LWR cladding performance by EPD surface modification technique*. Final report of NEUP project 09-766. Madison: University of Wisconsin, 2012.
[11] Bang I.C., Chang S.H. Boiling heat transfer performance and phenomena of Al_2O_3 – water nano-fluids from a plane surface in a pool. *International Journal of Heat and Mass Transfer*, 2005, **48**, P. 2407–2419.
[12] Vassalo P., Kumar R., D'Amigo S. Pool boiling heat transfer experiments in silica-water nano-fluids. *International Journal of Heat and Mass Transfer*, 2004, **47**, P. 407–411.
[13] Kim S.J., Bang I.C., Buongiorno J., Hu L.-W. Surface wettability change during pool boiling of nanofluids and its effect on critical heat flux. *International Journal of Heat and Mass Transfer*, 2007, **50**, P. 4105–4116.
[14] B.S. Fokin, M.Ya. Belenkiy, V.I. Almjashev, V.B. Khabensky, O.V. Almjasheva, V.V. Gusarov, Critical heat flux in a boiling aqueous dispersion of nanoparticles. *Technical Physics Letters*, 2009, **35**(5), P. 440–442.
[15] Kwark S.M., Moreno G., Kumar R. [et al]. Nanocoating characterization in pool boiling heat transfer of pure water. *International Journal of Heat and Mass Transfer*, 2010, **53**, P. 4579–4587.
[16] Kleinstreuer C., Feng Yu. Experimental and theoretical studies of nanofluid thermal conductivity enhancement: a review. *Nanoscale Research Letters*, 2011, **6**(229), P. 1–13.
[17] Rudyak V.Ya., Belkin A.A.. Tomilina E.A. On the thermal conductivity of nanofluids. *Technical Physics Letters*, 2010, **36**(7), P. 660–662.
[18] Surtaev A.S., Serdyukov V.S., Pavlenko A.N. Nanotechnologies for thermophysics: Heat transfer and crisis phenomena at boiling. Nanotechnologies in Russia, 2016, **11**(11-12), P. 696–715.
[19] Theofanous T.G., Dinh T.N. High heat flux boiling and burnout as microphysical phenomena: mounting evidence and opportunities. *Multiphase Science Tech*, 2006, **18**(1), P. 361–364.